

Four-loop results for the anomalous dimension for a general $N = 2$ supersymmetric Chern-Simons theory in three dimensions

I. Jack¹ and C. Luckhurst²

Dept. of Mathematical Sciences, University of Liverpool, Liverpool L69 3BX, UK

Abstract

We present results for the planar contribution to the four-loop anomalous dimension for a general $N = 2$ supersymmetric Chern-Simons theory in three dimensions. These results should facilitate higher-order superconformality checks for theories relevant for the AdS/CFT correspondence.

¹dij@liv.ac.uk

²mf0u60d7@liv.ac.uk

1 Introduction

Chern-Simons gauge theories have attracted attention for a considerable time due to their topological nature [1–3] (in the pure gauge case) and their possible relation to the quantum Hall effect and high- T_c superconductivity. More recently there has been substantial interest in $\mathcal{N} = 2$ supersymmetric Chern-Simons matter theories in the context of the AdS/CFT correspondence and in particular, a wide range of superconformal theories has been discovered [4]–[29], starting with the BLG [8, 9] and ABJ/ABJM [12, 24] models. Although a more familiar formulation is in terms of “quiver”-type gauge theories, many of them may be understood in terms of an underlying “3-algebra” structure [8], [30]–[38]. Explicit perturbative computations to corroborate the superconformal property have been carried out in Refs. [32, 39, 40] at lowest order (two loops for a theory in three dimensions). Since the gauge coupling is unrenormalised for any Chern-Simons theory due to the topological nature of the theory, it is only necessary to compute the anomalous dimensions of the chiral fields in order to check for superconformality (in view of the non-renormalisation theorem). Our purpose here is to provide results to enable the extension of this check to the next (four-loop) order. As may readily be imagined, this is a highly non-trivial undertaking. Consequently we envisage an abridged version of the full task. Firstly, we have calculated only the planar diagrams, corresponding to the leading N contributions. Even then, and even after discarding large classes of diagrams which can be seen in advance not to contribute to the anomalous dimension, one is faced with of the order of a hundred distinct diagrams. The process of automation which has made it feasible to perform high-loop calculations in non-supersymmetric theories using packages such as MINCER is not available to us here; we are not aware of any available package for performing superspace calculations. Secondly, therefore, we have confined ourselves to computing the coefficients of only a subset (albeit a large one) of the invariants contributing to the anomalous dimension. We believe that the remaining coefficients may be established by *assuming* the superconformality of a small number of the known examples of such theories. Armed with the full planar result, one could then continue to check the remaining ones, together with any new examples proposed in future. To put it another way, the conditions required for four-loop superconformality of all the known examples of such theories will form a highly redundant set of consistency conditions. Our lack of knowledge of all the coefficients in the anomalous dimension at this order will reduce this redundancy somewhat but there should be enough remaining to give considerable confidence in the persistence of the superconformality property to this order. Moreover we have tried to facilitate an extension of the check to include further invariants in the anomalous dimension, in the following sense: for the subset of invariants on which we have focussed our attention, we have (of course) computed all the diagrams which can contribute. Many of these diagrams also contribute to other invariants, and in these cases we have listed the contributions to these other invariants so that they can readily be combined with the contributions from the remaining diagrams at a later date.

The paper is organised as follows: in Section 2 we describe the general $\mathcal{N} = 2$ supersymmetric Chern-Simons theory in three dimensions; in Section 3 we describe our calculations

and give our result; Section 4 is devoted to a discussion of the result and suggestions for future work; while we explain our conventions and list various useful basic results and identities in an Appendix.

2 $\mathcal{N} = 2$ Chern-Simons theory in three dimensions

The action for the theory can be written

$$S = S_{SUSY} + S_{GF} \quad (1)$$

where S_{SUSY} is the usual supersymmetric action [41]

$$\begin{aligned} S_{SUSY} = & \int d^3x \int d^4\theta \left(k \int_0^1 dt \text{Tr}[\bar{D}^\alpha (e^{-tV} D_\alpha e^{tV})] + \Phi^j (e^{V_A R_A})^i_j \Phi_i \right) \\ & + \left(\int d^3x \int d^2\theta W(\Phi) + \text{h.c.} \right). \end{aligned} \quad (2)$$

Here V is the vector superfield, Φ the chiral matter superfield and the superpotential (quartic for renormalisability in three dimensions) $W(\Phi)$ is given by

$$W(\Phi) = \frac{1}{4!} Y^{ijkl} \Phi_i \Phi_j \Phi_k \Phi_l. \quad (3)$$

(We use the convention that $\Phi^i = (\Phi_i)^*$.) We assume a simple gauge group, though we comment later on the extension to non-simple groups. Gauge invariance requires the gauge coupling k to be quantised, so that $2\pi k$ is an integer. The vector superfield V is in the adjoint representation, $V = V_A T_A$ where T_A are the generators of the fundamental representation, satisfying

$$\begin{aligned} [T_A, T_B] &= i f_{ABC} T_C, \\ \text{Tr}(T_A T_B) &= \delta_{AB}. \end{aligned} \quad (4)$$

The chiral superfield can be in a general representation, with gauge matrices denoted R_A satisfying

$$\begin{aligned} [R_A, R_B] &= i f_{ABC} R_C, \\ \text{Tr}(R_A R_B) &= T_R \delta_{AB}. \end{aligned} \quad (5)$$

In three dimensions the Yukawa couplings Y^{ijkl} are dimensionless and (as mentioned earlier) the theory is renormalisable. In Eq. (1) the gauge-fixing term S_{GF} is given by [40]

$$S_{GF} = \frac{k}{2\alpha} \int d^3x d^2\theta \text{tr}[f \bar{f}] - \frac{k}{2\alpha} \int d^3x d^2\bar{\theta} \text{tr}[f \bar{f}] \quad (6)$$

and we introduce into the functional integral a corresponding ghost term

$$\int \mathcal{D}f \mathcal{D}\bar{f} \Delta(V) \Delta^{-1} V \quad (7)$$

with

$$\Delta(V) = \int d\Lambda d\bar{\Lambda} \delta(F(V, \Lambda, \bar{\Lambda}) - f) \delta(\bar{F}(V, \Lambda, \bar{\Lambda}) - \bar{f}), \quad (8)$$

with $\bar{F} = D^2 V$, $F = \bar{D}^2 V$. With $\alpha = 0$ this results in a gauge propagator

$$\langle V^A(1) V^B(2) \rangle = -\frac{1}{K} \frac{1}{\partial^2} \bar{D}^\alpha D_\alpha \delta^4(\theta_1 - \theta_2) \delta^{AB}. \quad (9)$$

The gauge vertices are obtained by expanding $S_{SUSY} + S_{GF}$ as given by Eqs. (2), (6):

$$\begin{aligned} S_{SUSY} + S_{GF} \rightarrow & -\frac{i}{6} f^{ABC} \int d^3 x d^4 \theta \bar{D}^\alpha V^A D_\alpha V^B V^C \\ & - \frac{1}{24} f^{ABE} f^{CDE} \int d^3 x d^4 \theta \bar{D}^\alpha V^A V^B D_\alpha V^C V^D + \dots \end{aligned} \quad (10)$$

The ghost action resulting from Eq. (8) has the same form as in the four-dimensional $\mathcal{N} = 1$ case [42, 43]

$$S_{gh} = \int d^3 x d^4 \theta \text{tr} \{ \bar{c}' c - c' \bar{c} + \frac{1}{2} (c + \bar{c}') [V, c + \bar{c}] + \frac{1}{12} (c + \bar{c}') [V, [V, c - \bar{c}]] + \dots \} \quad (11)$$

leading to ghost propagators

$$\langle \bar{c}'(1) c(2) \rangle = -\langle c'(1) \bar{c}(2) \rangle = -\frac{1}{\partial^2} \delta^4(\theta_1 - \theta_2). \quad (12)$$

and cubic, quartic vertices which may easily be read off from Eq. (11). Finally the chiral propagator and chiral-gauge vertices are readily obtained by expanding Eq.(2); the chiral propagator is given by:

$$\langle \Phi^i(1) \Phi_j(2) \rangle = -\frac{1}{\partial^2} \delta^4(\theta_1 - \theta_2) \delta^i_j. \quad (13)$$

The regularisation of the theory is effected by replacing V , Φ , Y by corresponding bare quantities V_B , Φ_B , Y_B , with the bare and renormalised fields related by

$$V_B = Z_V V, \quad \Phi_B = Z_\Phi \Phi. \quad (14)$$

Since the Chern-Simons level k is expected to be unrenormalised for a generic Chern-Simons theory due to the topological nature of the theory (so that $k_B = k$), superconformality will be determined purely by the vanishing of the β -functions for the superpotential coupling. These will be given according to the non-renormalisation theorem by

$$\beta_Y^{ijkl} = \gamma_{\Phi_m}^{(i} Y^{jkl)m}. \quad (15)$$

where the anomalous dimension γ_Φ is defined by

$$\gamma_\Phi = \mu \frac{d}{d\mu} \ln Z_\Phi. \quad (16)$$

Writing

$$Z_\Phi = \sum_{L \text{ even}, m=1 \dots \frac{L}{2}} \frac{Z_\Phi^{(L,m)}}{\epsilon^m} \quad (17)$$

γ_Φ is determined by the simple poles in Z_Φ according to

$$\gamma_\Phi^{(L)} = L Z_\Phi^{(L,1)} \quad (18)$$

and the higher order poles in Z_Φ are determined by consistency conditions, the one relevant for our purposes being

$$Z_\Phi^{(4,2)} = \beta_Y^{(2)} \cdot \frac{\partial}{\partial Y} \gamma_\Phi^{(2)} - 2 \left(\gamma_\Phi^{(2)} \right)^2 \quad (19)$$

where β_Y is given by Eq. (15) and

$$\beta_Y \cdot \frac{\partial}{\partial Y} \equiv \beta_Y^{klmn} \cdot \frac{\partial}{\partial Y^{klmn}}. \quad (20)$$

At lowest order (two loops) it was found that superconformality (i.e. the vanishing of β_Y) was equivalent to the vanishing of γ_Φ in all the cases considered [32, 40] and it appears likely that this will remain true at higher orders.

3 Perturbative Calculations

In this section we review the two-loop calculation and describe in detail our four-loop results.

The anomalous dimension of the chiral superfield is given at two loops by [32, 40]

$$(8\pi)^2 \gamma_\Phi^{(2)} = \frac{1}{3} Y_2 - 2k^{-2} C_R C_R - k^{-2} T_R C_R + k^{-2} C_G C_R \quad (21)$$

where

$$\begin{aligned} (Y_2)^i_j &= Y^{iklm} Y_{jklm} \\ C_R &= R_A R_A, \\ C_G \delta_{AB} &= f_{ACD} f_{BCD} \end{aligned} \quad (22)$$

and T_R is defined in Eq. (5). This result may readily be obtained by $\mathcal{N} = 2$ superfield methods [32, 40, 44, 45]; see the Appendix for our $\mathcal{N} = 2$ superfield conventions. Henceforth we set $k = 1$ for simplicity; it may easily be restored if desired. Two-loop results for general Chern-Simons theories have also been obtained in Ref. [46] but are not directly comparable since they were computed in the $N = 1$ framework.

As explained earlier, in this paper we confine ourselves to the contributions to the four-loop anomalous dimension from planar diagrams. From a consideration of possible group

invariants, the four-loop anomalous dimension is expected to take the form

$$\begin{aligned}
(8\pi)^4 \gamma_{\Phi}^{(4)} = & \alpha_1 Z_1 + \alpha_2 Z_2 + \alpha_3 W_1 + \alpha_4 W_2 + \alpha_5 W_3 + \alpha_6 W_4 + (\alpha_7 X + \alpha_8 C_G) U_1 \\
& + (\alpha_9 X + \alpha_{10} C_G) U_2 + \alpha_{11} C_{40} + \alpha_{12} C_{31} + \alpha_{13} C_{22} + \alpha_{14} C_{13} + \alpha_{15} F_4 \\
& + X (\alpha_{16} C_{30} + \alpha_{17} C_{21} + \alpha_{18} C_{12}) + X^2 (\alpha_{19} C_{20} + \alpha_{20} C_{11}) + \alpha_{21} X^3 C_R \\
& + \alpha_{22} X_2 + \alpha_{23} X_4 + (\alpha_{24} X + \alpha_{25} C_R + \alpha_{26} C_G) X_1 \\
& + \alpha_{27} X_5 C_R + (\alpha_{28} X + \alpha_{29} C_G) X_5 + \alpha_{30} X_3 \\
& + \alpha_{31} \text{tr}(C_R \{R_A, R_B\} R_C) R_A R_B R_C + \alpha_{32} X_6 + \alpha_{33} d_{CDA} d_{CDB} R_A R_B \quad (23)
\end{aligned}$$

where the invariants involving Yukawa couplings are given by

$$\begin{aligned}
(Y_3)^i_j &= Y^{ikmn} (Y_2)^l_k Y_{jlmn}, \\
(Y_4)^i_j &= Y^{iklr} Y_{klmn} Y^{mnpq} Y_{pqrj}, \\
Z_1 &= Y_2 C_R C_R, \\
(Z_2)^i_j &= Y^{iklm} Y_{jklm} (C_R C_R)^n_m, \\
(W_1)^i_j &= Y^{iklm} Y_{rknp} (R_A)^n_l (R_B)^p_m (R_A R_B)^r_j, \\
(W_2)^i_j &= Y^{iklm} Y_{pklm} (R_A R_B)^n_m (R_B R_A)^p_j, \\
(W_3)^i_j &= Y^{ikmp} Y_{jklm} (R_A R_B)^l_m (R_A R_B)^n_p, \\
(W_4)^i_j &= Y^{iklm} Y_{pklm} (R_A C_R)^n_m (R_A)^p_j, \\
U_1 &= Y_2 C_R, \\
(U_2)^i_j &= Y^{iklm} Y_{jklm} (C_R)^m_n, \quad (24)
\end{aligned}$$

and the remaining ones are

$$\begin{aligned}
C_{mn} &= C_R^m C_G^n, \\
F_4 &= f_{EAB} f_{ECD} f_{HAF} f_{HCG} R^B R^D R^F R^G, \\
X &= T_R - \frac{1}{2} C_G \\
X_1 &= \text{tr}(C_R R_A R_B) R_A R_B, \\
X_2 &= \text{tr}(R_A R_B R_C R_D) R_A R_B R_C R_D, \\
X_3 &= \text{tr}(C_R C_R R_A R_B) R_A R_B, \\
X_4 &= \text{tr}(Y_2 R_A R_B) R_A R_B, \\
X_5 &= D_{ABC} R_A R_B R_C, \\
X_6 &= f_{EAB} D_{ECD} R_A R_C R_B R_D, \quad (25)
\end{aligned}$$

with

$$D_{ABC} = \frac{1}{2} \text{tr}(\{R_A, R_B\} R_C). \quad (26)$$

The quantity X in Eq. (25) is produced by one-loop vector two-point insertions as depicted in Fig. 1. One can show using results from Ref. [47] that the structure X_6 vanishes for the

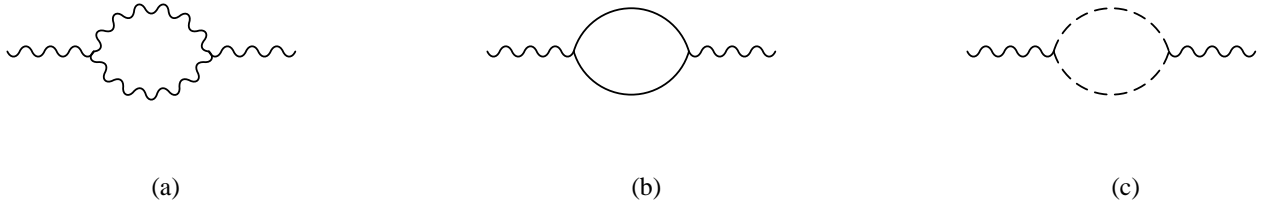


Figure 1: The one-loop insertions contributing to X

case of the fundamental representation; but we have not been able to prove this in general. We have decided to omit the computation of the coefficients $\alpha_{14,15}$, α_{18} , α_{20} , α_{26} , α_{29} and α_{30-33} , and therefore we shall leave out those diagrams which can only contribute to these coefficients. Our rationale broadly speaking has been to avoid coefficients which derive contributions from large numbers of diagrams. This typically entails avoiding invariants with factors of C_G , since it is clear for instance from Table 1 that invariants with more factors of C_G can arise from a larger number of diagrams. The coefficients $\alpha_{12,13}$, α_{17} are exceptions to this; we computed these since the corresponding invariants C_{31} , C_{22} and XC_{21} have non-zero double poles (see Eq. (30)), which we wished to compute as a consistency check.

We are therefore concerned with the calculation of two-point diagrams. We have used the package *FeynArts* [51] to assist in generating the full set of diagrams. This package requires as an input the basic four-loop planar vacuum topologies, since only the topologies up to three loops are contained in the standard package. The topologies which we have used in *FeynArts* are depicted in Fig. 2 and also in Fig. 7; the remaining topologies consist of insertions of loops on simple three-loop topologies and we have enumerated diagrams in these classes “by hand”. We can provide the topology files upon request to anyone interested in checking or extending our calculations.

Two large classes of diagrams may be immediately discarded as having no logarithmic divergences and therefore no contribution to the anomalous dimension [45]. The first consists of those diagrams in which the first (last) vertex encountered along the incoming (outgoing) chiral line has a single gauge line. These are shown schematically in Fig. 3(a). The second class consists of those diagrams which contain a one-loop subdiagram with one gauge and one chiral line; depicted in Fig. 3(b). We were able to use the features of *FeynArts* to discard such diagrams of the type in Fig. 3(a) automatically.

Instead of displaying each of the divergent graphs pictorially, which would be very laborious, we introduce a notation for various classes of diagram and illustrate it by means of representative examples, depicted in Fig. 4. The main exception is the graphs with Yukawa vertices, which we shall describe shortly. The majority of our graphs have no Yukawa vertices and most can be described using a fairly uniform notation. We start with graphs which have only a single chiral line, and only gauge/chiral vertices. The gauge-chiral vertices along the chiral line are labelled numerically in order from left to right. The structure of the diagram is then indicated by recording to which other vertices each vertex is connected, again from left to right. An example is depicted in Fig. 4(a).

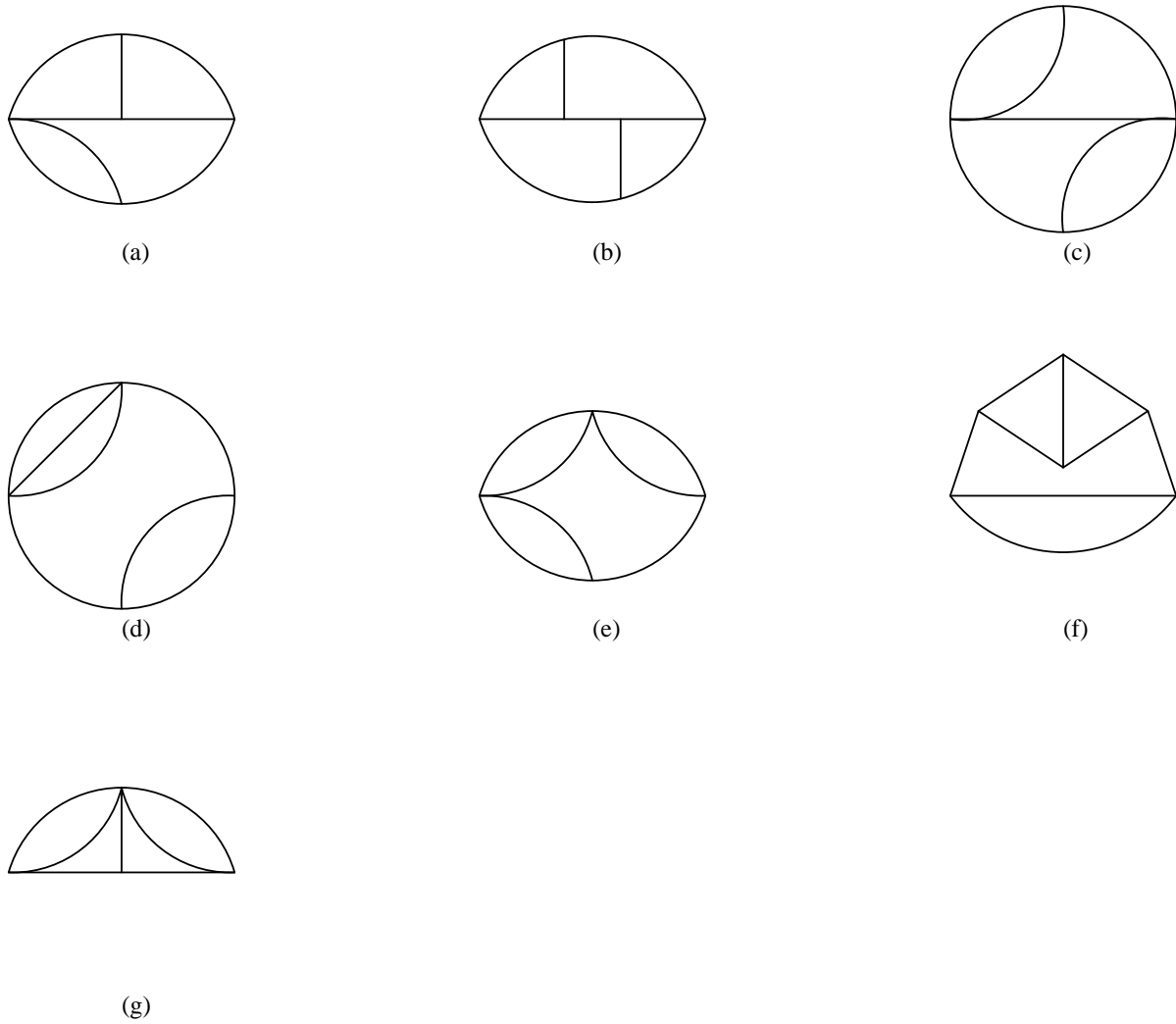
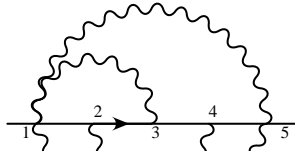


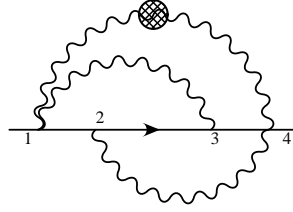
Figure 2: Four-loop topologies



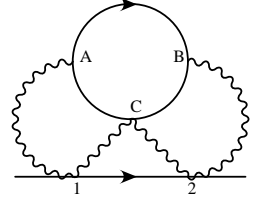
Figure 3: Classes of diagram which do not contribute



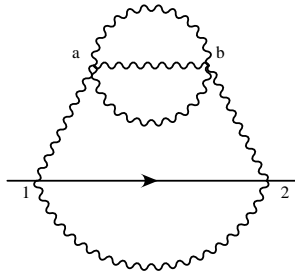
(a): (355)412(11)



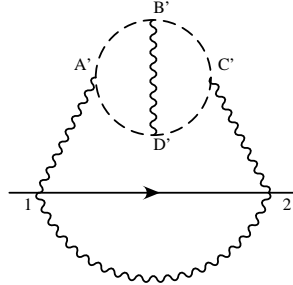
(b): (34)41(12) X_{14}



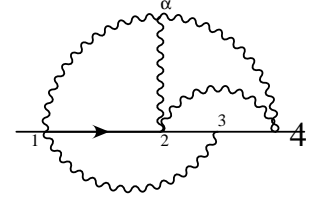
(c): (AC)(CB)



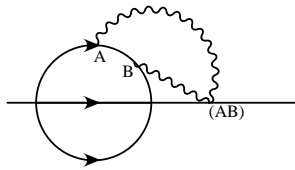
(d): (2a)(1b){(1b)(2a)}



(e): (2A')(1C'){1D'2B'}



(f): ($\alpha 3$)($\alpha 4$)1(2 α)



(g): [AB][][](AB)

Figure 4: Typical diagrams with their notation

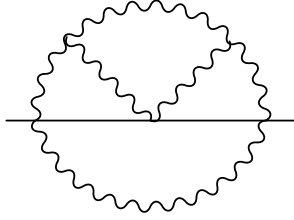


Figure 5: The additional graph from Table 5



Figure 6: The graphs of Table 9

The insertion of a one-loop gauge 2-point function on the propagator joining vertices i and j is denoted by the addition of X_{ij} ; see Fig. 4(b). More complex chiral loops (but without internal lines) are described by labelling the vertices on the loop by A , B , alphabetically, following the direction of the chiral arrows, and listing their connections to the vertices on the “main” chiral line as in the previous examples; as in Fig. 4(c). Gauge loops are described similarly, but with lower-case letters. If there are internal lines within the loop, these are denoted by listing the connections alphabetically in the same way as the main chiral line, but enclosed within brackets $\{\}$, as in Fig. 4(d). Ghost loops are denoted by labelling their vertices with primed letters, as in Fig. 4(e). Gauge vertices which do not lie within loops are denoted by greek letters and their connections with the main line or with loops denoted as usual, as in Fig. 4(f). A single graph which does not fall into any of these categories is that shown in Fig. 5 (the result for this graph will be given in Table 5).

Now we come to the graphs with Yukawa vertices. There are two graphs with four Yukawa vertices (and no gauge lines). Their structure can easily be derived from the corresponding group invariant (one for each graph). They will therefore simply be labelled by their group structure (Y_3 and Y_4 , as defined in Eq. (24)). The graphs with two Yukawa vertices (connected to an external line) and two gauge lines are described using a somewhat different notation to the above. The gauge matrices on chiral lines are labelled A , B , etc and the matrices on each chiral line in the chiral loop are enclosed within square brackets $[]$. Two matrices labelled with the same letter are connected by a gauge propagator. This is exemplified in Fig. 4(g). Finally, we have found it simplest to depict the diagram explicitly for a small class of diagrams with two Yukawa vertices, in Fig. 6.

Several diagrams clearly give no contribution by virtue of group theoretic considerations. For each remaining diagram the D -algebra is performed using the conventions and useful identities listed in the Appendix. A large number (almost all, in fact) of diagrams containing 3-point gauge vertices yield vanishing contributions when the results

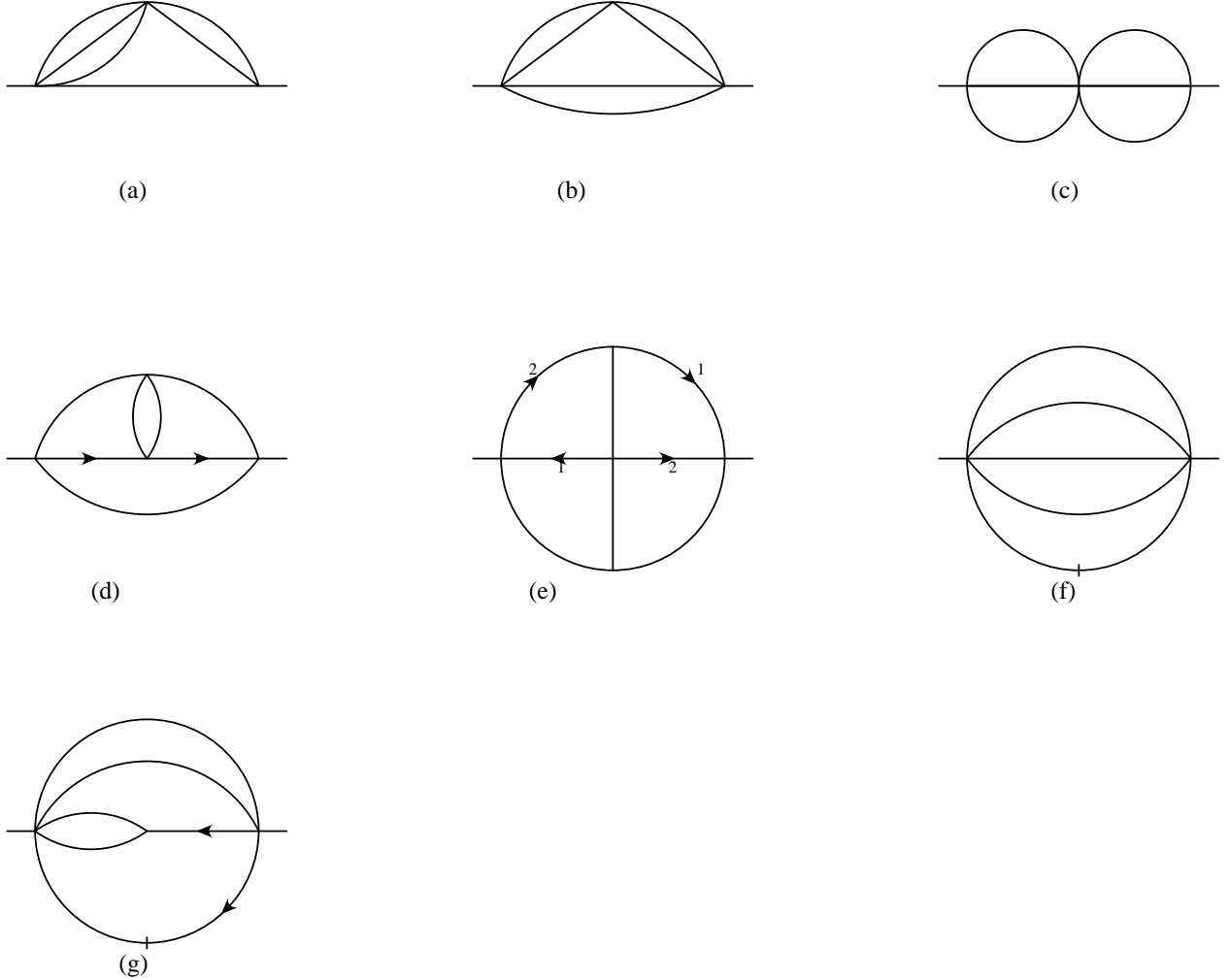


Figure 7: The basis of momentum integrals

of all possible arrangements of the D s and \overline{D} s are added together. Unfortunately we have not succeeded in establishing a criterion to predict in advance which diagrams give non-vanishing results. Our results for the non-vanishing divergences are listed diagram-by-diagram in Tables 3-13. Note that the graph $(3\alpha)\alpha\alpha(1\alpha)$ in Table 5 yields two distinct group structures which have been listed separately, the second occurrence distinguished by a prime.

Let us now explain how the Tables have been constructed. The results have been expressed in terms of a relatively small basis of momentum integrals [48, 49] which are depicted in Fig. 7 and whose divergences are also listed in the Appendix. Figs. 7(a)-(g) depict I_4 , I_{4bbb} , I_{22} , I_{42bbc} , $I_{422qAbBd}$, J_4 and J_5 , respectively. The results given later, and also most of these conventions for labelling the diagrams, are taken from Refs. [48, 49]. In Fig. 7 the arrows denote momenta in the numerator contracted as indicated. These momentum integrals multiply a variety of group structures, which appear in the final

columns of Tables 3-13. In Table 1 we give the decompositions of some of these group structures into the basis of group invariants. The definitions of these group structures are not given explicitly as they may easily be read off from the structure of the diagrams where they appear. Two examples should suffice: for instance, to take the diagrams Fig. 4(a), (b) respectively

$$\begin{aligned} S_4 &= R_{(A}R_BR_C)R_DR_AR_DR_{(B}R_C) \\ S_{X4} &= XR_{(A}R_BR_C)R_AR_{(B}R_C). \end{aligned} \quad (27)$$

Finally the first columns of Tables 3-13 contain an overall symmetry factor. The resulting contribution to the two-point function for each diagram is therefore obtained by adding the momentum integrals with the coefficients listed in the appropriate row and multiplying the resulting sum by the corresponding symmetry factor and group structure. For instance, the fourth row of Table 3 denotes a contribution

$$(-1)(-2I_4 + I_{4bbb}) \left(W_2 - \frac{1}{12}C_G U \right). \quad (28)$$

The combination of momentum integrals

$$\frac{1}{4}I_4 - \frac{5}{8}I_{22} - I_{4bbb} + I_{42bbc} - 2I_{422qAbBd}, \quad (29)$$

which one frequently observes in the tables, results from a momentum integral corresponding to the topology Fig. 7(e), but with a trace over a product of “ $p_{\alpha\beta}$ ” around the perimeter (constructed as in Eq. (39), where p is the momentum on one of the perimeter lines).

The first check on our results is provided by the consistency conditions Eq. (19) for the double poles. These, with the aid of Eq. (21), give

$$\begin{aligned} (8\pi)^4 Z_\Phi^{(4,2)} &= \frac{1}{6}Y_3 - \frac{1}{12}Z_1 + \frac{1}{4}Z_2 + \frac{1}{8} \left(U_2 - \frac{1}{3}U_1 \right) \left(X - \frac{1}{2}C_G \right) \\ &+ \frac{1}{2}C_{40} - \frac{1}{4}C_{31} + \frac{1}{32}C_{22} + \frac{1}{2}XC_{30} - \frac{1}{8}XC_{21} + \frac{1}{8}X^2C_{20}. \end{aligned} \quad (30)$$

We have checked all these non-zero coefficients, and moreover we have verified that the double poles for the remaining invariants whose coefficients we are computing vanish as they should. Of course the double pole contributions can in principle come from non-planar as well as planar diagrams. However, one can check that the only double-pole contribution from a non-planar diagram to one of the group structures whose divergent contribution we have computed is that from the diagram Fig. 8 (which contributes to α_{22}). Indeed, diagrams with three-point gauge vertices only have simple poles and the majority of non-planar diagrams are of this type. Including this double-pole contribution along with those from the planar diagrams in Table. 13, we find that the double pole proportional to X_2 in Eq. (25) is indeed cancelled. Of course the double poles corresponding to the invariants with coefficients $\alpha_{14,15}$, α_{18} , α_{20} , α_{26} , α_{29} and α_{30-33} should also cancel, but this we have not checked.

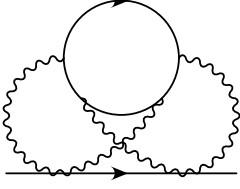


Figure 8: The non-planar graph

We note that the diagrams listed in Table 12 consist of insertions of a two-loop contribution to the gauge two-point function. These would be relevant to a superspace calculation of the corrections to the Chern-Simons level k ; also required would be the similar contributions to the ghost two-point function; and the two-loop corrections to the $V\bar{\Phi}\Phi$ vertex. Such calculations have been performed in components [50], but there may be some interest in corroborating them in the superspace context.

Our final result for the four-loop anomalous dimension is

$$\begin{aligned}
(8\pi)^4 \gamma_{\Phi}^{(4)} = & \frac{2}{3}Y_3 + \frac{\pi^2}{4}Y_4 - \frac{4}{3}Z_1 + \left(4 - \frac{2}{3}\pi^2\right)(4W_1 - Z_2) \\
& + \left(8 - \frac{5}{3}\pi^2\right)W_2 - \frac{1}{3}\pi^2W_3 + \frac{2}{3}\pi^2W_4 \\
& + \left[2\left(1 - \frac{1}{8}\pi^2\right)X - \left(1 - \frac{1}{4}\pi^2\right)C_G\right]\left(\frac{1}{3}U_1 - U_2\right) \\
& - 4(6 + \pi^2)C_{40} + \left(32 + \frac{17}{6}\pi^2\right)C_{31} - \frac{1}{2}\left(25 + \frac{23}{24}\pi^2\right)C_{22} \\
& + \alpha_{14}C_{13} + \alpha_{15}F_4 + X\left[-(8 + 3\pi^2)C_{30} + \left(2 + \frac{19}{6}\pi^2\right)C_{21} + \alpha_{18}C_{12}\right] \\
& + X^2[-(2 + \pi^2)C_{20} + \alpha_{20}C_{11}] - \frac{1}{8}\pi^2X^3C_R + \left(16 - \frac{7}{3}\pi^2\right)X_2 \\
& - \frac{2}{3}X_4 + [(8 - 3\pi^2)X - 2\pi^2C_R + \alpha_{26}C_G]X_1 + \frac{16\pi^2}{3}X_5C_R \\
& + (-\pi^2X + \alpha_{29}C_G)X_5 + \alpha_{30}X_3 + \alpha_{31}\text{tr}(C_R\{R_A, R_B\}R_C)R_AR_BR_C \\
& + \alpha_{32}X_6 + \alpha_{33}d_{CDAD}d_{CDB}R_AR_B.
\end{aligned} \tag{31}$$

As we explained in the introduction, we believe that the remaining undetermined coefficients may be determined by comparison with a small number of the known superconformal theories.

	C_{40}	C_{31}	C_{22}	C_{13}	F_4
S_1	1	$-\frac{1}{2}$	$\frac{1}{16}$	0	0
S_2	1	$-\frac{3}{2}$	$\frac{41}{48}$	$-\frac{33}{192}$	$\frac{5}{24}$
S_3	1	$-\frac{3}{4}$	$\frac{1}{8}$	0	0
S_4	1	$-\frac{5}{4}$	$\frac{13}{24}$	$-\frac{1}{12}$	0
S_5	1	$-\frac{3}{2}$	$\frac{5}{6}$	$-\frac{47}{288}$	$\frac{7}{36}$
S_6	1	-2	$\frac{65}{48}$	$-\frac{29}{96}$	$\frac{5}{12}$
S_7	1	$-\frac{5}{2}$	$\frac{33}{16}$	$-\frac{17}{32}$	1
S_8	1	-1	$\frac{3}{8}$	$-\frac{7}{128}$	$\frac{1}{16}$
S_9	1	$-\frac{3}{2}$	$\frac{13}{16}$	$-\frac{5}{32}$	$\frac{1}{4}$
S_{10}	1	$-\frac{5}{4}$	$\frac{9}{16}$	$-\frac{3}{32}$	$\frac{1}{8}$
S_{11}	1	$-\frac{7}{4}$	$\frac{33}{32}$	$-\frac{13}{64}$	$\frac{1}{4}$
S_{12}	1	$-\frac{3}{2}$	$\frac{3}{4}$	$-\frac{1}{8}$	0
S_{13}	1	$-\frac{3}{2}$	$\frac{3}{4}$	$-\frac{1}{8}$	$\frac{1}{16}$
S_{14}	1	$-\frac{7}{4}$	1	$-\frac{3}{16}$	$\frac{1}{8}$
S_{15}	1	$-\frac{21}{12}$	$\frac{103}{96}$	$-\frac{43}{192}$	$\frac{7}{24}$
S_{16}	1	-2	$\frac{21}{16}$	$-\frac{9}{32}$	$\frac{1}{4}$
S_{17}	1	$-\frac{9}{4}$	$\frac{27}{16}$	$-\frac{13}{32}$	$\frac{5}{8}$
S_{18}	0	1	$-\frac{11}{8}$	$\frac{7}{16}$	-1
S_{19}	0	1	$-\frac{7}{8}$	$\frac{3}{16}$	0
S_{20}	0	0	1	$-\frac{3}{8}$	2
S_{21}	0	0	$\frac{3}{2}$	$-\frac{5}{8}$	1
S_{22}	0	0	2	-1	2
S_{23}	0	0	$\frac{1}{2}$	$-\frac{1}{4}$	2
S_{24}	0	0	1	$-\frac{7}{18}$	$\frac{4}{3}$

Table 1: Decompositions into group invariants for diagrams of type Fig. 4(a)

	C_{30}	C_{21}	C_{12}
S_{X1}	1	$-\frac{3}{4}$	$\frac{1}{6}$
S_{X2}	1	$-\frac{7}{12}$	$\frac{5}{48}$
S_{X3}	1	$-\frac{3}{4}$	$\frac{5}{32}$
S_{X4}	1	-1	$\frac{1}{4}$
S_{X5}	1	$-\frac{1}{4}$	0
S_{X6}	0	1	$-\frac{3}{8}$

Table 2: Decompositions into group invariants for diagrams of type Fig. 4(b)

	I_4	I_{22}	I_{4bbb}	I_{42bbc}	$I_{422qAbBd}$		
Y_3	$\frac{1}{12}$	1	0	0	0	Y_3	
Y_4	$\frac{1}{8}$	0	0	1	0	Y_4	
$[A][B]\square(AB)$	-1	$-\frac{7}{4}$	$-\frac{5}{8}$	1	1	-2	W_1
$[AB]\square(AB)$	-1	-2	0	1	0	0	$W_2 - \frac{1}{12}C_G U$
$[(AB)]\square(AB)$	$\frac{1}{2}$	-2	0	0	0	0	$W_2 - \frac{1}{12}C_G U_1$
$[(AB)(AB)]\square\square$	$\frac{1}{4}$	-2	0	0	0	0	$Z_2 - \frac{1}{4}C_G U_2$
$[(AB)][(AB)]\square$	$\frac{1}{4}$	0	0	-2	0	0	$W_3 - \frac{1}{4}C_G U_2 + \frac{1}{12}C_G U_1$
$[A][(AB)][B]\square$	$-\frac{1}{2}$	$\frac{1}{4}$	$-\frac{5}{8}$	-1	1	-2	$\frac{1}{2}W_2 - W_3 + W_4 + \frac{1}{2}Z_2$
$[(AB)][AB]\square$	-1	$\frac{1}{4}$	$-\frac{5}{8}$	-1	1	-2	$W_3 - \frac{1}{4}C_G U_2 + \frac{1}{12}C_G U_1$
$[ABAB]\square\square$	$\frac{1}{2}$	0	0	1	0	0	$Z_2 - \frac{1}{2}C_G U_2$
$[ABA][B]\square$	1	$-\frac{1}{4}$	$\frac{5}{8}$	1	-1	2	$-\frac{1}{2}Z_2 + \frac{1}{4}C_G U_2 - \frac{1}{12}C_G U_1$
$(AB)\square\square\square(AB)$	$\frac{1}{12}$	-2	0	0	0	0	$Z_1 - \frac{1}{4}C_G U_1$
$[AA]\square\square X_{AA}$	$\frac{1}{2}$	1	0	$-\frac{1}{2}$	0	0	$X(U_1 - \frac{1}{2}U_2)$
$[A][A]X_{AA}$	$\frac{1}{2}$	0	$\frac{1}{2}$	0	0	0	XU_2
$[(AA)]\square\square X_{AA}$	$-\frac{1}{2}$	0	$\frac{1}{2}$	0	0	0	XU_2

Table 3: Results for diagrams of type Fig. 4(g)

4 Conclusions

As we stated in the introduction, it should be possible to exploit our results in Eq. (31) in order to verify the superconformality properties of various superconformal theories, as given explicitly either in terms of a “quiver” description or using 3-algebra structures. Our results (presented for the case of an ordinary simple gauge group) may require some adaptation in order to cast them in one or other of these forms; but we believe that this should be possible by inspection of the diagrammatic structure, in view of the fact that we have made no assumptions beyond standard group commutation relations in reducing our results to a standard basis of invariants. The “quiver” description is based on $U(N)$ (rather than $SU(N)$), and therefore identities such as those in Eq. (51) which we have used in our reduction to a basis of invariants, would require some modification, as detailed for instance in Ref. [52]; but these changes would have no effect at leading N , to which we are restricted anyway owing to our focus on planar diagrams. Given the large number of available candidates for superconformal theories, we expect that specialisation of our results to these various cases will provide compelling evidence for the superconformality at this highly non-trivial order.

One possible subtlety is the fact that renormalisation-group quantities such as the anomalous dimension are scheme-dependent beyond lowest order. This means that in principle one might have to adjust the couplings order by order so as to achieve finiteness

	I_4	I_{22}	I_{4bbb}	I_{42bbc}	$I_{422qAbBd}$	
(44)(33)(22)(11)	$\frac{1}{4}$	4	0	0	0	S_1
(233)(13)(112)	$-\frac{1}{2}$	0	0	4	0	S_5
(66)4523(11)	$\frac{1}{2}$	0	0	-2	0	S_3
(355)412(11)	-1	0	0	-2	0	S_4
(24)(13)(24)(13)	1	0	0	-2	0	S_8
(36)516(14)	1	0	0	0	-2	S_9
(25)(14)52(13)	-2	0	0	-1	0	S_{10}
(35)4(15)2(13)	-1	0	0	0	-2	S_{11}
(46)6513(12)	2	$-\frac{1}{4}$	$\frac{5}{8}$	0	-1	S_{12}
(34)(34)(12)(12)	1	0	0	-1	2	S_{13}
(35)(45)12(12)	-2	0	0	-1	2	S_{14}
(223)(113)(12)	-1	4	0	0	0	S_5
(234)(14)1(12)	2	0	0	1	0	S_{15}
(334)4(11)(12)	1	4	0	-2	0	S_6
(345)511(12)	-2	$\frac{1}{4}$	$-\frac{5}{8}$	0	1	S_6
(2233)(11)(11)	$-\frac{1}{2}$	4	0	0	0	S_2
(33)(44)(11)(22)	$\frac{1}{4}$	0	4	0	0	S_7
(22)(1133)(22)	$-\frac{1}{4}$	0	4	0	0	S_2
(33)4(114)(23)	1	0	2	0	0	S_6
(34)51(15)(24)	-2	-2	1	1	0	S_{14}
(23)(14)(14)(23)	1	-2	1	0	0	S_{13}
(35)6161(24)	1	$-\frac{5}{2}$	$\frac{9}{4}$	2	-2	S_{16}
(34)5(15)1(23)	-1	-2	1	2	0	S_{17}
(34)(55)11(22)	-1	0	2	0	0	S_7
(45)6611(23)	1	-2	1	2	0	S_7
(3 α)(4 α)1(2 α)	1	$-\frac{3}{4}$	$-\frac{1}{8}$	0	1	S_{18}
(5 α)4 α 2(1 α)	-1	$-\frac{1}{8}$	$\frac{5}{16}$	1	-1	S_{19}

Table 4: Results for diagrams of type Fig. 4(a),(f)

		I_4	I_{22}	I_{4bbb}	I_{42bbc}	$I_{422qAbBd}$	
$(\alpha\alpha)(3\alpha)(2\alpha)$	$\frac{1}{24}$	1	$\frac{1}{2}$	0	0	0	S_{20}
$(3\alpha\alpha)\alpha(1\alpha)$	$\frac{1}{72}$	0	0	$-\frac{1}{2}$	0	0	S_{21}
$(3\alpha)(\alpha\alpha)(1\alpha)$	$-\frac{1}{192}$	0	0	-4	-4	0	S_{20}
$(3\alpha)\alpha\alpha(1\alpha)$	$\frac{1}{24}$	$\frac{1}{2}$	$-\frac{5}{4}$	-1	3	-4	S_{20}
$(3\alpha)\alpha\alpha(1\alpha)'$	$\frac{1}{8}$	$-\frac{1}{4}$	$\frac{5}{8}$	0	-1	2	F_4
$(ab)(ab)(ab)$	$-\frac{1}{4}$	$\frac{5}{8}$	$-\frac{9}{16}$	-1	$\frac{1}{2}$	-1	S_{22}
$(\alpha\alpha)4\alpha(2\alpha)$	$-\frac{1}{12}$	0	0	$\frac{1}{2}$	0	0	S_{23}
$(3\alpha\alpha)(1\alpha\alpha)$	$\frac{1}{48}$	0	0	1	0	0	S_{24}
Fig. 5	$-\frac{1}{8}$	-1	$\frac{1}{2}$	0	0	0	S_{20}

Table 5: Results for graphs with 4-point gauge vertex and graphs of type Fig. 4(c),(d)

		I_4	I_{22}	I_{4bbb}	I_{42bbc}	$I_{422qAbBd}$	
$(3A)C(1B)\{132\}$	1	0	0	0	-1	0	$X_5C_R + \frac{1}{4}T_R(C_{21} - \frac{3}{8}C_{12})$
$(3A)B(1C)\{123\}$	1	$\frac{1}{2}$	$-\frac{5}{4}$	-1	2	-4	$X_5C_R - \frac{1}{4}T_R(C_{21} - \frac{3}{8}C_{12})$
$(3A')C'(1B')\{132\}$	$\frac{1}{16}$	0	0	0	-1	0	$C_{22} - \frac{3}{8}C_{13}$
$(3A')B'(1C')\{123\}$	$-\frac{1}{16}$	$\frac{1}{2}$	$-\frac{5}{4}$	-1	2	-4	$C_{22} - \frac{3}{8}C_{13}$
$(A3)A(B1)\{(12)3\}$	-2	0	0	$-\frac{1}{2}$	0	0	X_5C_R
$(AB2)(C1)\{112\}$	-2	-2	0	0	0	0	$X_5(C_R - \frac{1}{3}C_G)$
$(AB2)(B1)\{1(12)\}$	2	-2	0	0	0	0	$X_5(C_R - \frac{1}{3}C_G)$
$(AA2)(B1)\{(11)2\}$	1	0	0	-2	0	0	$X_5(C_R - \frac{1}{3}C_G)$
$(3A)B(1A)\{(13)2\}$	-1	0	0	0	-1	0	$X_5(C_R - \frac{3}{8}C_G)$

Table 6: Results for graphs contributing to X_5C_R , and similar topologies

	I_4	I_{22}	I_{4bbb}	I_{42bbc}	
$(222)(111)X_{12}$	-1	1	0	0	XS_{X1}
$(1122)(11)X_{11}$	-1	0	1	0	XS_{X2}
$(33)(22)(11)X_{22}$	$\frac{1}{2}$	0	1	0	XS_{X5}
$(233)1(11)X_{12}$	2	0	$\frac{1}{2}$	0	XS_{X1}
$(44)32(11)X_{23}$	-1	0	$\frac{1}{2}$	0	XS_{X5}
$(2a)(1a)X_{aa}$	$\frac{1}{6}$	0	1	0	XC_{21}
$(23)(13)(12)X_{12}$	-4	$\frac{1}{2}$	$-\frac{1}{4}$	0	XS_{X3}
$(23)(13)(12)X_{13}$	-1	0	0	1	XS_{X3}
$(34)41(12)X_{14}$	1	0	0	$\frac{1}{2}$	XS_{X4}
$(34)41(12)X_{13}$	2	1	$-\frac{1}{2}$	$-\frac{1}{2}$	XS_{X4}
$(\alpha 3)\alpha(\alpha 1)X_{\alpha 2}$	$-\frac{1}{2}$	-1	$\frac{1}{2}$	$\frac{1}{2}$	XS_{X6}

Table 7: Results for diagrams of type Fig. 4(b)

	I_4	I_{22}	I_{4bbb}	I_{42bbc}	J_4	J_5	
$(AB)\{(1B)(1A)\}X_{AB}$	$-\frac{1}{2}$	2	0	0	2	2	$X(X_1 - \frac{1}{4}C_G T_R C_R)$
$(AB)\{(1B)(1A)\}X_{1A}$	-1	2	0	0	0	0	$X(X_1 - \frac{1}{4}C_G T_R C_R)$
$(AC)\{(1B)A1\}X_{AB}$	1	0	1	0	1	1	$X(X_1 - \frac{1}{4}C_G T_R C_R)$
$(AB)\{(1C)1A\}X_{AC}$	1	0	1	0	1	1	$X(X_1 - \frac{1}{4}C_G T_R C_R)$
$(AD)\{1CB1\}X_{BC}$	-1	0	1	0	1	1	$X(X_1 - \frac{1}{2}C_G T_R C_R)$
$(AC)\{1D1B\}X_{BD}$	$-\frac{1}{2}$	-2	2	1	-2	0	$X(X_1 - \frac{1}{2}C_G T_R C_R)$
$(AC)\{1D1B\}X_{1A}$	-1	-2	0	1	0	0	$X(X_1 - \frac{1}{4}C_G T_R C_R)$
$(AC)\{1(BB)1\}X_{BB}$	1	0	2	0	0	0	XX_1
$(AB)\{(1AA)1\}X_{AA}$	1	0	-2	0	0	0	$X(X_1 - \frac{1}{2}C_G T_R C_R)$

Table 8: Results for diagrams contributing to XX_1

	I_4	J_4	I_{42bbc}	
Fig. 6(a)	$\frac{1}{12}$	2	-2	$X_4 C_R$
Fig. 6(b)	$-\frac{1}{6}$	1	-1	$X_4 C_R$

Table 9: Results for diagrams contributing to $X_4 C_R$

	I_4	I_{22}	I_{4bbb}	
$(11)(11)X_{11}X_{11}$	$-\frac{1}{8}$	0	1	$X^2(C_{20} - \frac{1}{6}C_{11})$
$(22)(11)X_{12}X_{12}$	$\frac{1}{2}$	$-\frac{1}{2}$	$\frac{1}{4}$	$X^2(C_{20} - \frac{1}{4}C_{11})$
$(22)(11)(X^2)_{12}$	1	0	0	$X^2(C_{20} - \frac{1}{4}C_{11})$
$(11)(X^3)_{11}$	$-\frac{1}{2}$	0	0	X^3C_R

Table 10: Results for diagrams contributing to $X^2C_R^2$ and X^3C_R

	I_4	I_{22}	I_{4bbb}	
$(ABC)X_{1A}$	1	1	0	XX_5
$(ABB)X_{1B}$	-1	1	0	XX_5
$(ABB)X_{1A}$	$-\frac{1}{2}$	0	1	XX_5

Table 11: Results for diagrams contributing to XX_5

	I_4	I_{4bbb}		
$(2a)(1b)\{(1b)(2a)\}$	$\frac{1}{24}$	1	0	$C_{22} - \frac{1}{4}C_{13}$
$(2A')(1B')\{(1B')(2A')\}$	$\frac{1}{6}$	1	0	$C_{22} - \frac{1}{4}C_{13}$
$(2A')(1C')\{1D'2B'\}$	$-\frac{1}{8}$	1	$-\frac{1}{2}$	$C_{22} - \frac{1}{4}C_{13}$
$(2A')(1\alpha)\{1\alpha\alpha\}$	$-\frac{1}{8}$	0	1	$C_{22} - \frac{1}{4}C_{13}$
$(2A)(1B)\{(1B)(2A)\}$	-2	1	0	$(X_1 - \frac{1}{4}C_G T_R C_R)(C_R - \frac{1}{4}C_G)$
$(2A)(1C)\{1D2B\}$	2	1	$-\frac{1}{2}$	$(X_1 - \frac{1}{4}C_G T_R C_R)(C_R - \frac{1}{4}C_G)$
$(2A)(1\alpha)\{1\alpha\alpha\}$	1	0	2	$\frac{1}{4}C_G T_R$

Table 12: Results for two-loop vector two-point insertion diagrams

		I_4	I_{22}	I_{4bbb}	I_{42bbc}	$I_{422qAbBd}$	
$(AB)(CD)$	1	-4	0	1	1	0	$X_2 - \frac{1}{16}T_R C_{12} + \frac{1}{2}C_G X_5$
$(AC)(BC)$	-1	-4	0	1	1	0	$X_2 - \frac{3}{32}T_R C_{12} + \frac{5}{8}C_G X_5 - \frac{1}{4}iX_6$
$(AB)(BC)$	-1	$-\frac{15}{4}$	$-\frac{5}{8}$	1	2	-2	$X_2 - \frac{3}{32}T_R C_{12} + \frac{5}{8}C_G X_5 - \frac{1}{4}iX_6$
$(AB)(AB)$	$\frac{1}{2}$	-4	0	1	2	0	$X_2 - \frac{3}{32}T_R C_{12} + \frac{5}{8}C_G X_5 - \frac{1}{4}iX_6$
$(AA)(BC)$	-1	-2	0	0	0	0	$X_2 - \frac{1}{16}T_R C_{12} + \frac{1}{2}C_G X_5$
$(AA)(AB)$	1	-2	0	0	0	0	$X_2 - \frac{3}{32}T_R C_{12} + \frac{5}{8}C_G X_5 - \frac{1}{4}iX_6$
$(ABCD)$	$-\frac{1}{4}$	$\frac{1}{4}$	$-\frac{5}{8}$	-1	1	-2	$X_2 - \frac{3}{32}T_R C_{12} + \frac{5}{8}C_G X_5 - \frac{1}{4}iX_6$
$(AABB)$	$-\frac{1}{8}$	0	0	4	0	0	$X_2 - \frac{3}{32}T_R C_{12} + \frac{5}{8}C_G X_5 - \frac{1}{4}iX_6$

Table 13: Results for diagrams contributing to X_2

[53, 54]. This could be accommodated by parametrising all possible redefinitions of the couplings. It is perhaps worth recalling that in four dimensions, the finiteness properties of $\mathcal{N} = 4$ and $\mathcal{N} = 2$ supersymmetric theories are manifest to all orders in the $\mathcal{N} = 1$ superfield description once the field content has been specified (assuming a supersymmetric regulator such as DRED). However, when finite $\mathcal{N} = 1$ theories are constructed, the finiteness is obtained through an order-by-order adjustment of the couplings. On the whole it seems to us likely that the superconformal situation in three dimensions will resemble the $\mathcal{N} = 4$ and $\mathcal{N} = 2$ situation in four dimensions in cases where exact, explicit formulations can be presented for the action, such as the BLG and ABJ/ABJM cases. However, in cases such as the superconformal theories conjectured to exist in Ref. [20] through a process of interpolation, and given explicitly only to lowest order in Ref. [40]; and indeed the whole range of superconformal theories found in Refs. [39], [40] by solving the lowest order conformal invariance conditions, order-by-order redefinitions of the couplings will be needed. The coupling redefinitions should merely result in a slight reduction of the large redundancy in the system of equations rising from requiring superconformality of the various candidate theories; and so the superconformality check will still be compelling.

Of course further weight would be given to any superconformality checks by continuing the computation of the remaining unknown coefficients in Eq. (31). This would be hugely simplified if we could understand in advance which diagrams with 3-point gauge vertices will yield a vanishing contribution. In any case the remainder of the computation is certainly not insuperable, merely somewhat laborious. The extension to the non-planar diagrams is also in principle feasible, though we do not at present have available a convenient basis of momentum integrals already tabulated for this case. On the other hand, many of the non-planar diagrams may not actually contribute since most of them will contain 3-point gauge vertices.

Acknowledgements

One of us (CL) was supported by a University of Liverpool studentship. IJ is grateful for useful discussions with Tim Jones.

Appendix

In this appendix we list our superspace and supersymmetry conventions. We use a metric signature $(+ - -)$ so that a possible choice of γ matrices is $\gamma^0 = \sigma_2$, $\gamma^1 = i\sigma_3$, $\gamma^2 = i\sigma_1$ with

$$(\gamma^\mu)_\alpha{}^\beta = (\sigma_2)_\alpha{}^\beta, \quad (32)$$

etc. We then have

$$\gamma^\mu \gamma^\nu = \eta^{\mu\nu} - i\epsilon^{\mu\nu\rho} \gamma_\rho. \quad (33)$$

We have [40] two complex two-spinors θ^α and θ_α with indices raised and lowered according to

$$\theta^\alpha = C^{\alpha\beta} \theta_\beta, \quad \theta_\alpha = \theta^\beta C_{\beta\alpha}, \quad (34)$$

with $C^{12} = -C_{12} = i$. We then have

$$\theta_\alpha \theta_\beta = C_{\beta\alpha} \theta^2, \quad \theta^\alpha \theta^\beta = C^{\beta\alpha} \theta^2, \quad (35)$$

where

$$\theta^2 = \frac{1}{2} \theta^\alpha \theta_\alpha. \quad (36)$$

The supercovariant derivatives are defined by

$$D_\alpha = \partial_\alpha + \frac{i}{2} \bar{\theta}^\beta \partial_{\alpha\beta}, \quad (37)$$

$$\bar{D}_\alpha = \bar{\partial}_\alpha + \frac{i}{2} \theta^\beta \partial_{\alpha\beta}, \quad (38)$$

where

$$\partial_{\alpha\beta} = \partial_\mu (\gamma^\mu)_{\alpha\beta}, \quad (39)$$

satisfying

$$\{D_\alpha, \bar{D}_\beta\} = i \partial_{\alpha\beta}. \quad (40)$$

We also define

$$d^2\theta = \frac{1}{2} d\theta^\alpha d\theta_\alpha \quad d^2\bar{\theta} = \frac{1}{2} d\bar{\theta}^\alpha d\bar{\theta}_\alpha, \quad d^4\theta = d^2\theta d^2\bar{\theta}, \quad (41)$$

so that

$$\int d^2\theta \theta^2 = \int d^2\bar{\theta} \bar{\theta}^2 = -1. \quad (42)$$

The vector superfield $V(x, \theta, \bar{\theta})$ is expanded in Wess-Zumino gauge as

$$V = i\theta^\alpha \bar{\theta}_\alpha \sigma + \theta^\alpha \bar{\theta}^\beta A_{\alpha\beta} - \theta^2 \bar{\theta}^\alpha \bar{\lambda}_\alpha - \bar{\theta}^2 \theta^\alpha \lambda_\alpha + \theta^2 \bar{\theta}^2 D, \quad (43)$$

and the chiral field is expanded as

$$\Phi = \phi(y) + \theta^\alpha \psi_\alpha(y) - \theta^2 F(y), \quad (44)$$

where

$$y^\mu = x^\mu + i\theta\gamma^\mu\bar{\theta}. \quad (45)$$

Here is the list of results for the divergences of our basis of momentum integrals [48, 49]:

$$I_4 = \frac{1}{(8\pi)^4} \left(-\frac{1}{2\epsilon^2} + \frac{2}{\epsilon} \right) \quad (46)$$

$$I_{22} = -\frac{1}{(8\pi)^4 \epsilon^2} \quad (47)$$

$$I_{4bbb} = \frac{1}{(8\pi)^4} \frac{\pi^2}{2\epsilon} \quad (48)$$

$$I_{42bbc} = \frac{1}{(8\pi)^4} \frac{2}{\epsilon} \quad (49)$$

$$I_{422qAbBd} = \frac{1}{(8\pi)^4} \left[\frac{1}{4\epsilon^2} + \frac{1}{\epsilon} \left(\frac{5}{4} - \frac{\pi^2}{12} \right) \right] \quad (50)$$

The table of group structures may be readily obtained using the following easily derived but useful group identities:

$$\begin{aligned}
R_B R_A R_B &= \left(C_R - \frac{1}{2} C_G \right) R_A, \\
f^{ABE} f^{CDE} R_A R_C R_B R_D &= 0, \\
R_A R_B R_C R_A R_B R_C &= C_{30} - \frac{3}{2} C_{21} + \frac{1}{2} C_{12}, \\
R_A R_B R_C R_D R_A R_B R_C R_D &= C_{40} - 3C_{31} + \frac{11}{4} C_{22} - \frac{3}{4} C_{13} + F_4, \\
R_A R_B R_C R_A R_D R_B R_C R_D &= C_{40} - \frac{5}{2} C_{31} + 2C_{22} - \frac{1}{2} C_{13} + F_4, \\
R_A R_B R_C R_D R_A R_C R_B R_D &= C_{40} - 2C_{31} + \frac{3}{2} C_{22} - \frac{3}{8} C_{13} + F_4, \\
f^{ABC} R_A R_D R_C R_E R_D R_B R_E &= -i \left(\frac{1}{2} C_{31} - \frac{3}{4} C_{22} + \frac{1}{4} C_{13} - F_4 \right), \\
f^{ABF} f^{CDF} R_A R_C R_E R_D R_B R_E &= \frac{1}{4} C_{22} - \frac{1}{8} C_{13} + F_4, \\
f^{ABF} f^{CDF} R_A R_C R_E R_B R_D R_E &= F_4, \\
f^{ABC} f^{DEF} R_A R_D R_B R_E R_C R_F &= -\frac{1}{4} C_{22} + \frac{1}{8} C_{13} - F_4
\end{aligned} \tag{51}$$

References

- [1] A.S. Schwarz, *Lett. Math. Phys.* **2** (1978) 247; *Commun. Math. Phys.* **67** (1979) 1
- [2] E. Witten, *Commun. Math. Phys.* **121** (1989) 351
- [3] S. Deser, R. Jackiw and S. Templeton, *Ann. Phys.* 140 (1982) 372
- [4] J.H. Schwarz, *JHEP* 0411 (2004) 078
- [5] H.C. Kao and K.M. Lee, *Phys. Rev.* **D46** (1992) 4691
- [6] I.L. Buchbinder, E.A. Ivanov, O. Lechtenfeld, N.G. Pletnev, I.B. Samsonov and B.M. Zupnik, *JHEP* 0910 (2009) 075
- [7] B.M. Zupnik and D.V. Khetselius, *Sov. J. Nucl. Phys.* 47 (1988) 730
- [8] J. Bagger and N. Lambert, *Phys. Rev.* **D75** (2007) 045020; *Phys. Rev.* **D77** (2008) 065008
- [9] A. Gustavsson, *Nucl. Phys.* **B811** (2009) 66
- [10] M. Van Raamsdonk, *JHEP* 0805 (2008) 105

- [11] M. Benna, I. Klebanov, T. Klose and M. Smedback, *JHEP* 0809 (2008) 072
- [12] O. Aharony, O. Bergman and D.L. Jafferis, *JHEP* 0811 (2008) 043
- [13] M. Schnabl and Y. Tachikawa, *JHEP* 1009 (2010) 103
- [14] D. Martelli and J. Sparks, *Phys. Rev.* **D78** (2008) 126005
- [15] A. Hanany and A. Zaffaroni, *JHEP* 0810 (2008) 111
- [16] S. Franco, A. Hanany, J. Park and D. Rodriguez-Gomez, *JHEP* 0812 (2008) 110
- [17] A. Hanany and Y.H. He, arXiv:0811.4044[hep-th]
- [18] E. Imeroni, *JHEP* 0810 (2008) 026
- [19] D.L. Jafferis and A. Tomasiello, *JHEP* 0810 (2008) 101
- [20] D. Gaiotto and A. Tomasiello, *JHEP* 1001 (2010) 015; *J. Phys* **A** 42 (2009) 465205
- [21] S. Hohenegger and I. Kirsch, *JHEP* 0904 (2009) 129
- [22] D. Gaiotto and D.L. Jafferis, arXiv:0903.2175[hep-th]
- [23] Y. Hikida, W. Li and T. Takayanagi, *JHEP* 0907 (2009) 065
- [24] O. Aharony, O. Bergman, D.L. Jafferis and J. Maldacena, *JHEP* 0810 (2008) 091
- [25] K. Hosomichi, K.L. Lee, S. Lee, S. Lee and J. Park, *JHEP* 0807 (2008) 091
- [26] E.A. Bergshoeff, O. Hohm, D. Roest, H. Samtleben and E. Sezgin, *JHEP* 0809 (2008) 101
- [27] K. Hosomichi, K.L. Lee, S. Lee, S. Lee and J. Park, *JHEP* 0809 (2008) 002
- [28] P. de Medeiros, J. Figueroa-O’Farrill, E. Mendez-Escobar and P. Ritter, *Comm. Math. Phys.* 290 (2009) 871902
- [29] P. de Medeiros, J. Figueroa-O’Farrill, E. Mendez-Escobar, *J. Phys.* **A42** (2009) 485204
- [30] J. Bagger and N. Lambert, *Phys. Rev.* **D79** (2009) 025002
- [31] F.-M. Chen and Y.-S. Wu, *Eur. Phys. J* **C69** (2009) 305
- [32] N. Akerblom, C. Saemann and M. Wolf, *Nucl. Phys.* **B826** (2010) 456
- [33] F.-M. Chen, *JHEP* 1008 (2010) 077
- [34] F.-M. Chen and Y.-S. Wu, *Phys. Rev.* **D82** (2010) 106012
- [35] F.-M. Chen and Y.-S. Wu, *JHEP* 1302 (2013) 016

- [36] J. Bagger and G. Bruhn, *Phys. Rev.* **D83** (2011) 025003
- [37] F.-M. Chen, *J. Math. Phys.* **53** (2012) 012301
- [38] F.-M. Chen and Y.-S. Wu, arXiv:1212.6650
- [39] M. S. Bianchi, S. Penati and M. Siani, *JHEP* 1001 (2010) 080
- [40] M.S. Bianchi, S. Penati and M. Siani, *JHEP* 1005 (2010) 106
- [41] E.A. Ivanov, *Phys. Lett.* **B268** (1991) 203
- [42] S.J. Gates, M.T. Grisaru, M. Rocek and W. Siegel, *Front. Phys.* **58** (1983) 1
[arXiv:hep-th/0108200]
- [43] M.T. Grisaru, M. Rocek and W. Siegel, *Nucl. Phys.* **B159** (1979) 429
- [44] L.V. Avdeev, G.V. Grigoryev and D.I. Kazakov, *Nucl. Phys.* **B382** (1992) 561
- [45] S.J. Gates and H. Nishino, *Phys. Lett.* **B72** (1992) 72
- [46] L.V. Avdeev, D.I. Kazakov and I.N. Kondrashuk, *Nucl. Phys.* **B391** (1993) 333
- [47] J.A. de Azcarraga, A.J. Macfarlane, A.J. Mountain and J.C. Perez Bueno, *Nucl. Phys.* **B510** (1998) 657
- [48] J.A. Minahan, O.O. Sax and C. Sieg, *Nucl. Phys.* **B846** (2011) 542
- [49] M. Leoni, A. Mauri, J.A. Minahan, A. Santambrogio, C. Sieg and G. Tartaglino-Mazzucchelli, *JHEP* 1012 (2010) 074
- [50] W. Chen, G.W. Semenoff and Y-S. Wu, *Phys. Rev.* **D46** (1992) 5521
- [51] T. Hahn, *Comput. Phys. Commun.* **140** (2001) 418
- [52] L. Bonora and M. Salizzoni, *Phys. Lett.* **B504** (2001) 80
- [53] D.R.T. Jones, *Nucl. Phys.* **B277** (1986) 153
- [54] A.V. Ermushev, D.I. Kazakov and O.V. Tarasov, *Nucl. Phys.* **B281** (1987) 72